

# Soft Matter

Accepted Manuscript



This is an *Accepted Manuscript*, which has been through the Royal Society of Chemistry peer review process and has been accepted for publication.

*Accepted Manuscripts* are published online shortly after acceptance, before technical editing, formatting and proof reading. Using this free service, authors can make their results available to the community, in citable form, before we publish the edited article. We will replace this *Accepted Manuscript* with the edited and formatted *Advance Article* as soon as it is available.

You can find more information about *Accepted Manuscripts* in the [Information for Authors](#).

Please note that technical editing may introduce minor changes to the text and/or graphics, which may alter content. The journal's standard [Terms & Conditions](#) and the [Ethical guidelines](#) still apply. In no event shall the Royal Society of Chemistry be held responsible for any errors or omissions in this *Accepted Manuscript* or any consequences arising from the use of any information it contains.

Cite this: DOI: 10.1039/xxxxxxxxxx

# Estimation of the Free Energy of Adsorption of a Polypeptide on Amorphous SiO<sub>2</sub> from Molecular Dynamics Simulations and Force Spectroscopy Experiments

Robert Horst Meißner,<sup>\*a</sup> Gang Wei,<sup>b</sup> and Lucio Colombi Ciacchi<sup>b,c</sup>

Received Date

Accepted Date

DOI: 10.1039/xxxxxxxxxx

www.rsc.org/journalname

Estimating the free energy of adsorption of materials-binding peptides is fundamental to quantify their interactions across bio/inorganic interfaces, but is difficult to achieve both experimentally and theoretically. We employ a combination of molecular dynamics (MD) simulations and dynamical force-spectroscopy experiments based on atomic force microscopy (AFM) to estimate the free energy of adsorption  $\Delta G_{\text{ads}}$  of a (GCRL) tetrapeptide on amorphous SiO<sub>2</sub> in pure water. The results of both equilibrium, advanced sampling MD and non-equilibrium, steered MD are compared with those of two different approaches used to extract  $\Delta G_{\text{ads}}$  from the dependence of experimentally measured adhesion forces on the applied AFM loading rates. In order to obtain unambiguous peak forces and bond loading rates from steered MD trajectories, we have developed a novel numerical protocol based on a piecewise-harmonic fit of the adhesion work profile along each trajectory. The interpretation of the experiments has required a thorough quantitative characterization of the elastic properties of polyethylene glycol linker molecules used to tether (GCRL)<sub>15</sub> polypeptides to AFM cantilevers, and of the polypeptide itself. All obtained  $\Delta G_{\text{ads}}$  values fall within a relatively narrow window between -5 and -9 kcal/mol, but can be associated with large relative error bars of more than 50%. Among the different approaches compared, Replica Exchange with Solute Tempering simulations augmented with Metadynamics (RESTMetaD) and fitting of dynamic force spectroscopy experiments with the model of Friddle and De Yoreo lead to the most reliable  $\Delta G_{\text{ads}}$  estimates.

## 1 Introduction

The interaction between biomolecules and solid surfaces has become of eminent interest in fields ranging from basic research up to industrial product design<sup>1,2</sup>. For instance, the development of pharmaceutical packaging for protein-based drugs relies on coating materials that inhibit protein adhesion on the packaging surfaces, and avoid conformational changes of the active components caused by surface adsorption. Anti-ice or anti-fouling coatings are also realized through the immobilization of proteins on solid substrates<sup>3-5</sup>, and novel biomimetic materials can be syn-

thesized by mineralization of short polypeptide sequences that selectively recognize and strongly bind to inorganic solid phases<sup>6-9</sup>. Therefore, experimental and simulation effort has been recently spent for a rationalization of the fundamental physical processes that govern the biomolecule-surface interactions at an atomic scale. In this context, several methods that are able to indirectly quantify the free energy of adsorption  $\Delta G_{\text{ads}}$  of short polypeptides on solid materials have been proposed<sup>10</sup>. However, an unambiguous, quantitative comparison between different methods, and especially between experiments and simulations, has been achieved only in rare cases<sup>11-14</sup>.

Experimental methods that can be used to estimate  $\Delta G_{\text{ads}}$  are for instance quartz-crystal microbalance with dissipation (QCM-D), surface plasmon resonance (SPR) spectroscopy<sup>15</sup>, or isothermal titration calorimetry (ITC), concomitantly with the application of adequate adsorption isotherm models, such as the one of Langmuir<sup>16</sup>. However, the applicability of SPR or QCM-D rarely goes beyond model systems, since they are limited to nanoscale-thick material coatings on a sensor chip<sup>17-20</sup>. Alternatively, force-

<sup>a</sup> Fraunhofer Institute for Manufacturing Technology and Applied Materials Research (IFAM), Wiener Str. 12, 28359 Bremen, Germany. Fax: +49 421 2246 300; Tel: +49 421 2246 380; E-mail: rmei@uni-bremen.de

<sup>b</sup> Hybrid Materials Interfaces Group, Faculty of Production Engineering, Bremen Center for Computational Materials Science and Center for Environmental Research and Sustainable Technology (UFT), University of Bremen, Bibliothekstraße 1, 28359 Bremen, Germany

<sup>c</sup> MAPEX Center for Materials and Processes, University of Bremen, Bibliothekstraße 1, 28359 Bremen, Germany

spectroscopy (FS) methods, for instance based on atomic force microscopy (AFM), can be employed, provided that a relationship between the directly measured adhesion forces and  $\Delta G_{\text{ads}}$  exist<sup>15,20,21</sup>. An advantage of AFM-based FS (briefly, AFM-FS) is that a variety of substrates and probe molecules can be investigated<sup>22,23</sup>. Moreover, several models have been proposed to explain the dependencies of the force required to break a chemical or physical bond (within a folded biomolecule, between a receptor and a ligand, or between a molecule and a surface) on the bond loading rate<sup>24–28</sup>. Indirectly, many of these models are able to provide estimates on  $\Delta G_{\text{ads}}$ , at least under a limited set of conditions, such as under small or large loading rates, or for negligible molecule/surface friction<sup>29,30</sup>. A comparison between different models applied to the case of the binding forces within an amyloid- $\beta$  fibre can be found in the work of Hane *et al.*<sup>30</sup>

A widely applied model has been introduced by Friddle *et al.*<sup>25</sup>, generalizing the initial approach of Evans and Ritchie<sup>24</sup> to take into account binding/rebinding equilibria and the presence of multiple bonds. Another approach, based on the original Bell and Evans model, takes into explicit account the contribution of flexible linker molecules to the loading rate<sup>26,27</sup>. Alternatively, the thermodynamics of the desorption event of long polypeptide molecules from solid/liquid interfaces substrates have been analyzed by various authors<sup>29,31–33</sup>. Particularly interesting is the analysis of Krysiak *et al.*<sup>29</sup>, since in their model the free energy of adsorption can be estimated without explicit knowledge of the contour length of the linker molecule, which is generally unknown. However, the conclusions of this work hold only for the case of frictionless substrates. Recently, Bullerjahn *et al.*<sup>34</sup> proposed a model which describes reasonably well the widespread spectra of low and high loading rates, which is particularly useful to analyze dynamic force spectra calculated theoretically by means of molecular dynamics simulations.

Simulations methods have also emerged only very recently as a viable way of predicting the adhesion forces and adsorption free energies at bio/inorganic interfaces<sup>12,35–38</sup>. Crucial to this regard has been the application of methods that thoroughly sample the conformational space during the adsorption/desorption process, such as the Hamiltonian Replica Exchange<sup>39</sup> and its variants<sup>40–42</sup>, alone or in combination with Metadynamics<sup>35,36,43,44</sup>. Furthermore, non-equilibrium simulation methods such as steered molecular dynamics (SMD) are able to reveal details of the actual reaction paths leading to the (constrained) detachment of biomolecules from solid surfaces. SMD simulations would thus be in principle directly comparable to AFM-FS experiments, if the bond loading rates applied in the experiments and simulations were the same. Unfortunately, this is not the case since the computational cost of the simulations only allows the molecule to be pulled off the surface at very high speed (of the order of 0.1 m/s or larger), and at reasonably large values of the harmonic spring constant of the pulling constraint. It is also to be noted that extracting equilibrium quantities such as adsorption free energies from non-equilibrium simulations can be an extremely difficult task<sup>45</sup>, because of the necessity of complete phase-space sampling. Therefore, the famous equality of Jarzynski, that calculates the equilibrium free-energy difference

between two states from the complete set of non-equilibrium work values associated with each individual trajectory that connects the same states, has had only limited practical applicability so far<sup>46</sup>.

In the present article we concentrate on a model system consisting of a tetrapeptide with sequence GCRL (glycine, cysteine, arginine and leucine)<sup>9</sup> interacting with an amorphous SiO<sub>2</sub> surface model at neutral pH, for which we have developed a realistic atomistic structure and an accurate force field in previous works<sup>47–50</sup>. The adsorption free energy  $\Delta G_{\text{ads}}$  is theoretically predicted using both equilibrium (Replica Exchange with Solute Tempering combined with Metadynamics, or briefly REST-MetaD<sup>44</sup>) and non-equilibrium (SMD) methods via Jarzynski's equality<sup>51</sup>. AFM-FS experiments at variable loading rates are then performed and the results interpreted with the models of Friddle<sup>25</sup> and Krysiak<sup>29</sup>/Paturej<sup>33</sup> to provide experimental free energy estimates. Beside comparing the values obtained via the experiments and simulations, our goal is to highlight the advantages and shortcomings of each of the methods employed.

## 2 Experimental

### 2.1 Force Spectroscopy Experiments

The force spectroscopy experiments are performed in a liquid cell using a NanoWizard NanoScience atomic force microscope (JPK Instruments AG, Berlin, Germany) with a functionalized Si<sub>3</sub>N<sub>4</sub> cantilever (DNP-S10, Bruker Corporation, France) of spring constant  $k_c = 0.42 \pm 0.08$  pN/Å, as determined via its resonance frequency and the equipartition method<sup>52,53</sup>. Prior to functionalization, the cantilever is cleaned in a freshly prepared Piranha solution for 30 min and washed repeatedly with water and ethanol. It is then immersed into a solution of 3-aminopropyl triethoxysilane (APTES) for 15 minutes and successively incubated in a solution containing a polyethylene glycol n-hydroxysuccinimide ester disulfide (PEG-NHS) and a O-Methyl-O'-[2-(succinylamino)ethyl]polyethylene glycol N-succinimidyl ester (PEG-Ome) in ratio of 1:20. The PEG-functionalized cantilever is then incubated in a solution containing 0.1 mg/mL (GCRL)<sub>15</sub> polypeptides (Sel-leck Chemicals LLC, Houston, USA), to attach them covalently through their amino terminal to the PEG-NHS linker only. The PEG-Ome linker serves as a spacer to reduce the number of polypeptides tethered to the cantilever tip to a few units, and to reduce the non-specific tip/surface interactions.

Force-displacement curves were collected in ultrapure water after purification with a Mill-Q Integral system against the surface of a fused quartz surface (Hellma Optics GmbH, Jena, Germany) previously cleaned with a Piranha solution and rinsed with abundant ethanol and water. The roughness of the surface, as determined by AFM imaging, amounted to  $0.29 \pm 0.01$  nm in areas of the order of  $2 \times 2 \mu\text{m}^2$ . The curves were collected in "force mapping" mode using sets of  $16 \times 16$  points per each retraction speed value (from 0.05 to 5  $\mu\text{m/s}$ ), a z-length of 0.4  $\mu\text{m}$ , an extend time of 0.8 s and a delay time on the substrate of 1 s. The reported data are the averages of all curves presenting a clear polypeptide/surface interaction plateau, out of three independent measurement sets. The data were analyzed with the JPK SPM Data

processing software (Version 4.3.11).

## 2.2 Molecular Dynamics Simulations

All MD simulations were carried out using the LAMMPS simulation package<sup>54</sup> utilizing the AMBER03 force field<sup>55,56</sup> in combination with the TIP3P water model<sup>57</sup>. Interactions between the silica surface, biomolecules and water are described using the recently published force field of Butenuth *et al.*<sup>50</sup>. The bulk silica is described by an own modified version of the potential of Demiralp *et al.*<sup>58</sup>, as described in detail in Meißner *et al.*<sup>36</sup>. The input structures for the (GCRL) and (GCRL)<sub>5</sub> peptides are generated using the LEaP suite of the AMBER software package. The deprotonation of a silica surface depends strongly on pH, ionic strength and particle diameter<sup>59,60</sup>. Taking into account the counterions inserted in our simulations to ensure charge neutrality of the complete system, the surface charge density at pH 7.0 and at a corresponding ionic strength amounts to about 0.55 e/nm<sup>2</sup><sup>59</sup>. This surface charge density is set by deprotonation of randomly chosen silanol terminal groups (cf. ref. 36).

The simulations based on Replica Exchange with Solute Tempering augmented with Metadynamics (RESTmetaD) are performed as reported in refs. 35 and 36, using a set of 7 independent replicas at temperatures ranging from 300 to 450 K with a  $\Delta T$  of 25 K. The well-tempered metadynamics algorithm acts on the center of mass position of the peptide by adding Gaussian hills with an initial height of 0.7 kcal/mol and a width of 0.1 Å every 0.5 ps to the corresponding bias potential. The Steered Molecular Dynamics (SMD) simulations are performed with the help of harmonic potentials of the form

$$V_c = \frac{k_c}{N} \cdot (d - d_0)^2, \quad (1)$$

where  $N$  is the number of constrained atoms,  $k_c$  is the spring constant of the constraint (or virtual AFM cantilever),  $d$  is the normal distance of the center of mass of the  $N$  atoms to the surface, and  $d_0$  is the variable height of the constraint over the surface, moving at constant speed. 45 random adsorbed configurations of the peptide are obtained by pushing the peptide towards the surface with a speed of 0.01 Å/ps, applying a constraint potential  $V_c$  with  $k_c = 9.5$  pN/Å on all peptide atoms, until a repulsive force between 500 and 1000 pN is reached. Desorption of the peptide is steered by inverting the constraint velocity direction, using several values of  $k_c$  and pulling speeds (vide infra), and applying  $V_c$  only to the C atom of the N-terminus of the peptide. Before desorption, the initial position of the harmonic constraint is carefully chosen in order to match the final repulsive force obtained in the constrained adsorption. Since the harmonic spring constants of the approach and retraction simulations differ, this requires particular care. This procedure effectively mimics the action of an AFM cantilever functionalized with single peptides.

## 3 Results and discussion

### 3.1 Free Energy of Adsorption from RESTmetaD simulations

In previous works, we have set the basis for accurate calculations of the free energy of adsorption of polypeptides on solid surfaces

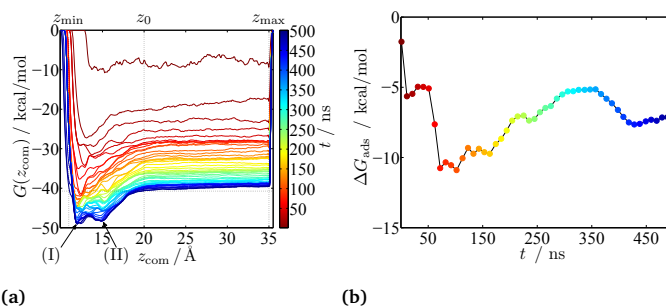


**Fig. 1** (a) Free energy profile the GCRL peptide absorbing onto an anionic silica surface as a function of the peptide's center of mass position  $z_{\text{com}}$  in direction perpendicular to the surface, calculated with RESTmetaD. The temporal evolution of the profile is indicated with colors from dark red to blue. (b) Temporal evolution of the free energy of adsorption  $\Delta G_{\text{ads}}$  obtained by Boltzmann integration of the corresponding profile within the limits given in (a), using eq. (2).

by means of Replica Exchange with Solute Tempering augmented with Metadynamics (RESTmetaD)<sup>35,36</sup>. In brief, we first compute the probabilities  $\rho_{\text{ads}}$  and  $\rho_{\text{dis}}$  of finding the peptide in an adsorbed or in a dissolved state, respectively, by Boltzmann integration of the one-dimensional free energy profile  $G(z_{\text{com}})$ , where the collective variable  $z_{\text{com}}$  represents the position of the peptide's center of mass in direction perpendicular to the surface. We then compute the free energy of adsorption as

$$\Delta G_{\text{ads}} = -k_B T \ln \left( \frac{\rho_{\text{ads}}}{\rho_{\text{dis}}} \right), \quad (2)$$

where  $k_B$  is the Boltzmann constant and  $T$  the temperature of the system. The evolution of  $G(z_{\text{com}})$  along a RESTmetaD trajectory of GCRL adsorbing on silica is shown in Fig. 1a, and allows us to define the position  $z_0 = 20.0$  Å as the border between the adsorbed state ( $z_{\text{min}} < z_{\text{com}} < z_0$ ) and the dissolved state ( $z_0 < z_{\text{com}} < z_{\text{max}}$ ), as defined in Fig. 1a. While the choice of  $z_0$  is arbitrary, it is important to guarantee that the free energy profile is flat in the dissolved state region, indicating that the peptide does not experience any surface interaction and behaves as in bulk solution. Under this condition,  $\Delta G_{\text{ads}}$  is practically not affected by small changes of the set  $z_0$  value.

The temporal evolution of  $\Delta G_{\text{ads}}$  during the RESTmetaD simulation is shown in Fig. 1b. After 500 ns, we reach a final value of -7.3 kcal/mol with an error of about 1.8 kcal/mol, estimated from the fluctuations of  $\Delta G_{\text{ads}}$  in the last 250 ns of simulation. We note that the development of two separate minima (labelled I and II in Fig. 1a) in the adsorbed state region takes place only after 350 ns of simulation, pointing towards the importance of long runs to capture essential details of the free energy landscape.

Representative molecular conformations associated with these minima are reported in Fig. 2.

In conformation I (Fig. 2a,b), all amino acids are in very close contact to the surface, forming hydrogen bonds with the terminal silanol groups. In particular, the positively charged side chain of the arginine residue neighbors a deprotonated silanol. In conformation II (Fig. 2c,d), the peptide assumes an upright position,

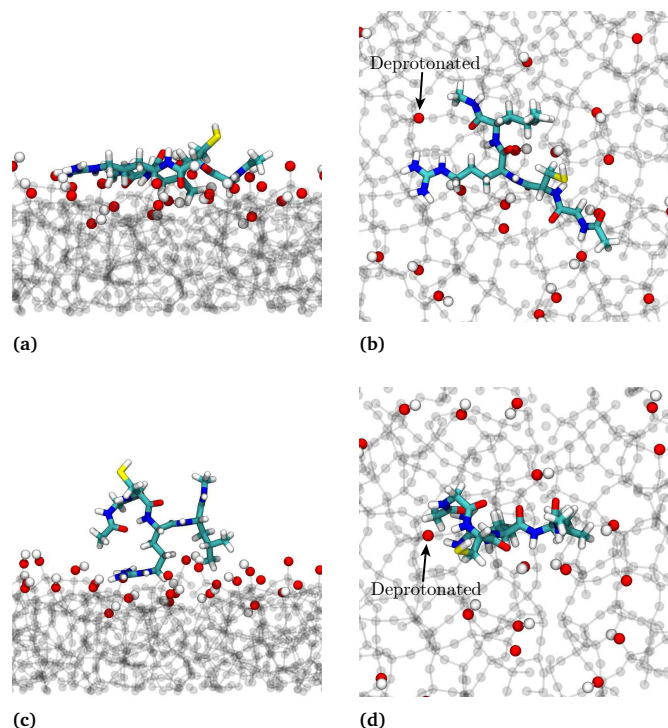


**Fig. 2** Side (a,c) and top (b,d) views of the molecular structures associated with the free energy minima (I) and (II) of Figure 1a at  $z_{\text{com}} = 12 \text{ \AA}$  (a,b) and  $15 \text{ \AA}$  (c,d).

keeping surface contact only via the C-terminus, the leucine and the arginine side chains. Notable is that both polar (and charged) and non-polar amino acid side chains contribute to surface adhesion, as we already noticed in other studies<sup>9,35,36,49,61</sup>. Also interesting is the fact that the -SH terminal group of cysteine in both cases remains fully hydrated, far from the surface.

### 3.2 Adsorption Forces and Free Energies from SMD Simulations

#### 3.2.1 Free Energy of Adsorption from Jarzynski's Equality

In the previous section, the calculation of  $\Delta G_{\text{ads}}$  relies on a complete sampling of the phase space and Boltzmann integration of the free energy profile, which is assumed to describe the thermodynamical equilibrium of the system after reaching convergence. Alternatively, as we show in the following, the free energy of adsorption can be estimated from force desorption spectra calculated by out-of-equilibrium steered molecular dynamics (SMD) simulation and application of Jarzynski's equality<sup>51</sup>

$$e^{-\Delta G/k_B T} = \overline{e^{-\Delta W/k_B T}}. \quad (3)$$

In this equation,  $\Delta G$  is the free energy difference between two states and  $\Delta W$  is the work necessary to bring the system from one state to the other. It is important to note that  $\Delta W$  must be calculated under non-equilibrium conditions, which guarantees correct weighting of individual SMD trajectories<sup>51</sup>. To this aim, we carry out an extensive set of SMD simulations pulling the GCRL molecule from an arbitrary adsorbed microstate (generated as described in the Methods) towards a desorbed microstate by means

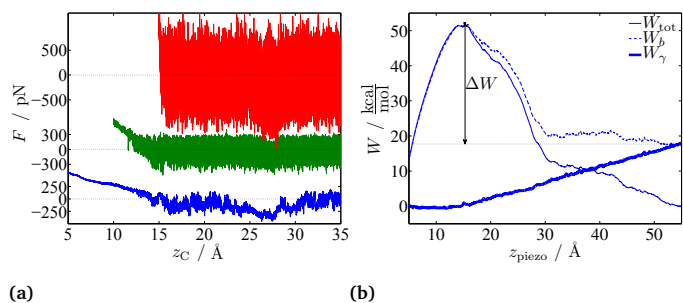


**Fig. 3** (a) SMD retraction curves of the GCRL peptide from the anionic silica surface using pulling speeds of 0.05 (blue), 0.005 (green) and 0.01  $\text{\AA}/\text{ps}$  (red) and spring constants of 69.48, 138.96 and 694.80  $\text{pN}/\text{\AA}$ , respectively. Forces are shifted in y-direction for readability. (b) Cumulative work (thin solid line) calculated from the blue retraction curve on the left. The frictional and desorption components to the total work are shown as thick solid and dashed lines, respectively.  $\Delta W$  denotes the desorption work used in Jarzynski's Equality.

of an harmonic constraint applied to the N-terminal C atom, moving with constant velocity in direction perpendicular to the surface. We perform a total of 810 SMD simulations using three different cantilever spring constants of 69.5, 139.0 and 694.8  $\text{pN}/\text{\AA}$ , and six pulling velocities  $v_{\text{pull}}$  ranging from 0.001 to 0.5  $\text{\AA}/\text{ps}$ .

Examples of the resulting force-distance curves are reported in Figure 3a and show large force fluctuations, scaling with the spring stiffness according to  $\sqrt{k_c k_B T}$ .<sup>62</sup> Cumulative numerical integration of these curves leads, nevertheless, to rather smooth work profiles (Fig 3b), from which  $\Delta W$  can be extracted unequivocally.

However, especially at high pulling velocity, a frictional contribution to the pulling force due to the motion of the molecule through the viscous water solvent becomes appreciable. This contribution should not enter into Jarzynski's equality if the equilibrium free energy of adsorption is sought for, since the latter is the energy barrier required to detach the molecule from the surface in the limit of zero pulling speeds.

In order to calculate this frictional contribution, we perform SMD simulations of the GCRL peptide dragged through a periodically repeated box of water with constant velocity  $v_{\text{drag}}$  using an harmonic spring with stiffness  $k_c = 69.5 \text{ pN}/\text{\AA}$  applied to the N terminal C atom. This enables us to perform arbitrarily long simulations without changing the pulling direction, provided that the linear and angular velocities of the centre of mass of all water molecules is zeroed after each MD step and the system temperature is kept constant via coupling to a Nosé-Hoover thermostat. The frictional coefficient can then be calculated either directly from the obtained average friction force  $\langle F_\gamma \rangle$  according to Stoke's law, or via the frictional work  $W_\gamma(z) = \frac{1}{z-z_0} \cdot \int_{z_0}^z F_\gamma \cdot dz'$  necessary to drag the peptide from a position  $z_0$  to a position  $z$ :

$$\gamma = \frac{\langle F_\gamma \rangle}{v_{\text{drag}}} = \frac{W_\gamma(z)}{\int_{z_0}^z v(z') \cdot dz'}, \quad (4)$$

where  $v(z)$  is the instantaneous velocity of the C atom to which the harmonic constraint is tethered. The obtained dragging forces and work profiles for  $v_{\text{drag}}$  values of 0.05, 0.1, 0.2, 0.3 and

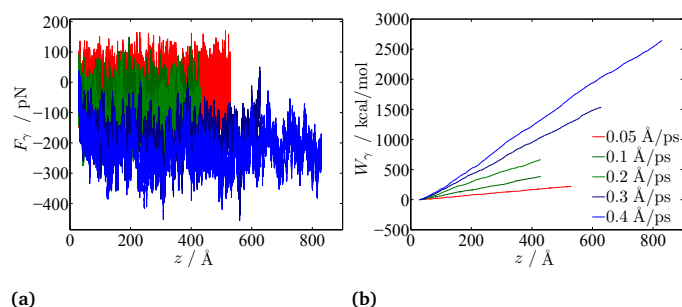


**Fig. 4** Frictional force (a) and work (b) versus path length of the GCRL peptide dragged through TIP3P water with five  $v_{\text{drag}}$  speeds indicated with different colors.

**Table 1** Friction coefficient  $\gamma$  for the GCRL peptide dragged through TIP3P water with five  $v_{\text{drag}}$  speeds.

$v_{\text{drag}} / (\text{Å}/\text{ps})$	$\gamma / (\text{pN}\cdot\text{ps}/\text{Å})$
0.05	612
0.1	670
0.2	579
0.3	593
0.4	576

0.4 Å/ps are reported in Fig. 4, and the calculated values of  $\gamma$  in Table 1.

We note that, if Stoke's law of friction holds,  $\gamma$  should be the same for all different dragging velocities. The variations evident in Table 1 are most probably due to the limited simulation times together with the large force fluctuations, which lead to errors in the average force and average work, especially at low dragging velocities. The molecular friction coefficient  $\gamma$  of the GCRL peptide in water is thus computed by averaging over all dragging velocity and amounts to  $606 \pm 39$  pN ps/Å.

We can now compute the molecular friction contributions  $W_\gamma$  present in the GCRL desorption work profiles by multiplying the velocity of the N-terminus C atom,  $v_C$ , with the molecular friction coefficient  $\gamma$ . This contribution is then subtracted from the work profile  $W_{\text{tot}}$  to obtain the pure desorption work  $W_b$ , from which the desorption barrier  $\Delta W$  entering into Jarzynski's equality can be obtained (see Fig. 3). As expected, the profiles obtained at  $v_{\text{pull}}$  below 0.01 Å/ps are hardly affected by the viscous friction, since the corresponding frictional work is smaller than about 0.2 kcal/mol.

To compute the free energy of adsorption, instead of using the pristine Jarzynski's equality (Eq. 3), we follow the approach of Park *et al.*<sup>63</sup>, which accounts for the effect of finite sampling. Using this approach, the free energy of adsorption is

$$\Delta G_{\text{ads}} = \frac{1}{M} \sum_{i=1}^M \Delta W_i - \frac{1}{2k_B T} \frac{M}{M-1} \left[ \frac{1}{M} \sum_{i=1}^M \Delta W_i^2 - \left( \frac{1}{M} \sum_{i=1}^M \Delta W_i \right)^2 \right], \quad (5)$$

where  $M$  is the number of individual SMD simulations for each  $k_c$  and  $v_{\text{pull}}$ . The obtained results are shown in Fig. 5.

As expected, as  $v_{\text{pull}}$  decreases, more and more precise estimates of  $\Delta G_{\text{ads}}$  are predicted by Eq. 5. Moreover, the convergence is faster for higher  $k_c$ , since Jarzynski's equality is exact only in

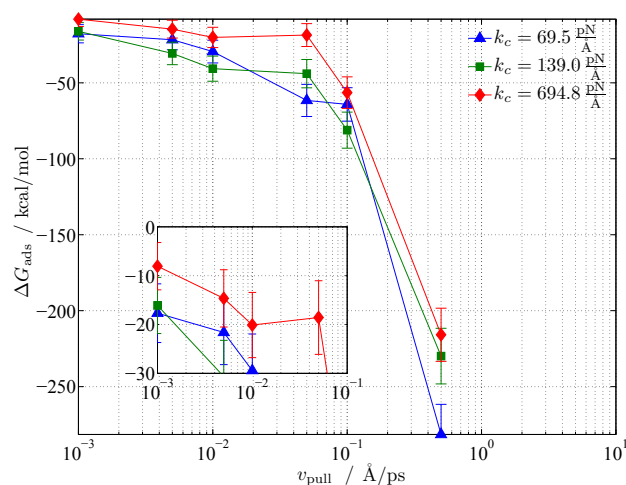


**Fig. 5** Free energy of adsorption  $\Delta G_{\text{ads}}$  obtained with Jarzynski's Equality applied to SMD data using different spring constants and pulling speeds. The inset in (b) magnifies the graphics region for low pulling speeds.

the limit of infinitely stiff springs, being the result of a Taylor expansion series of the potential of mean force in this limit<sup>63</sup>. In practice, however, too high  $k_c$  values are associated with too large fluctuations (see Fig. 3), which are a source of error in the estimates of  $\Delta W$ . For the stiffest harmonic constraint used here, we obtain an estimated  $\Delta G_{\text{ads}} = -8.0 \pm 4.9$  kcal/mol, corresponding reasonably well to the value of -7.3 kcal/mol obtained in the RESTmetaD simulation. The error of about 5 kcal/mol is defined by the work fluctuation  $\sqrt{\langle \Delta W^2 \rangle - \langle \Delta W \rangle^2}$  in each set of SMD trajectories with the same  $k_c$  and  $v_{\text{pull}}$ , which is often used as a measure of the applicability of Jarzynski's equality<sup>51,64,65</sup>. This relatively large error is mostly due to the insufficient sampling, but is comparable with the error bar of the other methods used here (vide infra), and can thus be considered acceptable for the purposes of the present work.

### 3.2.2 Applying the Model proposed by Friddle to SMD Force Retraction Curves

Extracting the free energy of adsorption from SMD pulling simulations at different speeds corresponds to performing dynamical force-spectroscopy experiments, typically with an Atomic Force Microscope (AFM). The influence of the loading rate on the desorption forces has been reported previously in several works<sup>25,66,67</sup>. When an external pulling force is applied to an adsorbed molecule, desorption takes place along a non-equilibrium energy path, which results in a logarithmic dependency of the desorption peak force on the loading rate. The effective loading rate  $r_{\text{eff}}$  is defined as the product of the pulling velocity  $v_{\text{pull}}$  and the effective spring constant  $k_{\text{eff}}$  acting on the surface-molecule bond;  $r_{\text{eff}} = v_{\text{pull}} \cdot k_{\text{eff}}$ . For soft enough effective spring constants, it follows from the Bell-Evans model that the free energy of adsorption can be obtained from<sup>25</sup>

$$\Delta G_{\text{ads}} = \frac{F_{\text{eq}}^2}{2 \cdot \langle k_{\text{eff}} \rangle}, \quad (6)$$

**Table 2** Fit parameters of harmonic potentials (Eq. 7) in the six regions of the SMD force-displacement curve defined in Figure 6.

$n$	$z_n^{\text{off}} / \text{\AA}$	$A_n / \frac{\text{kcal}}{\text{mol}}$	$k_n / \frac{\text{pN}}{\text{\AA}}$
I	14.6	26.3	-33.9
II	18.7	24.1	-42.0
III	22.6	15.9	-58.9
IV	24.0	9.5	-16.3
V	27.2	2.3	-3.3

where  $F_{\text{eq}}$  is the limit of the average desorption peak force for zero loading rates. In the following, we attempt to apply the model of Friddle<sup>25</sup> to our computed SMD data, although we are well aware that the pulling velocities in the simulations are several orders of magnitude higher than the ones in typical AFM force-spectroscopy experiments.

A problem that we immediately encounter is that the large force fluctuations blur out the force peaks. To overcome this problem we propose here an automatic procedure to identify desorption peaks based on a piecewise-linear approximation of the force-distance curves (Fig. 6). Firstly, the force-distance curves are smoothed with a moving average filter using a Gaussian window of 1 Å width, and the smoothed force,  $F_{\text{smooth}}$ , is numerically differentiated with respect to the path length  $z_C$  (Fig. 6a). The positions of the maxima of the force derivative correspond to the positions at which individual surface-molecule bonds successively break during the pulling process. The original force profile is then cumulatively integrated over  $z_C$ , leading to a smooth desorption work profile  $W(z_C)$  (Fig. 6b). The work profile in each region  $n$  between two successive bond breaking events at positions  $z_n^{\text{low}}$  and  $z_n^{\text{high}}$  (as identified previously) is nearly harmonic and can thus be least-square fitted by a function

$$W_n(z) = \begin{cases} -k_n \cdot (z - z_n^{\text{off}})^2 + A_n, & \text{for } z_n^{\text{low}} < z < z_n^{\text{high}} \\ 0, & \text{elsewhere} \end{cases} \quad (7)$$

The fitting parameters in each harmonic potential region are the effective spring constant  $k_n$ , the distance offset  $z_n^{\text{off}}$ , and the energy offset  $A_n$  (see Table 2)

A piecewise-harmonic work profile corresponding to the whole desorption process can be now obtained by  $W_{\text{fit}}(z_C) = \sum_{i=1}^{\max(n)} W_i(z_C)$  (Fig. 6c). Finally, a piecewise-linear force profile (Fig. 6d) is obtained upon derivation:

$$F_{\text{fit}}(z_C) = -\frac{d}{dz_C} W_{\text{fit}}(z_C). \quad (8)$$

In the example shown in Fig. 6, the SMD force-distance curve can be approximated by five linear segments, each corresponding to a bond breaking event, until complete desorption of the peptide takes place (region VI).

Using this fitting procedure we can now identify the maximum desorption force and its corresponding effective bond stiffness  $k_{\text{eff}}$  (i.e. the slope of the linear segment preceding the peak) in each of the 810 SMD simulations performed. A mean effective stiffnesses  $\langle k_{\text{eff}} \rangle$  for each of the three  $k_c$  values (69.5, 139.0 and 694.8 pN/Å) is calculated from a log-normal distribution fitted to the histogram of all individual  $k_{\text{eff}}$  values (Figure 7a). A log-

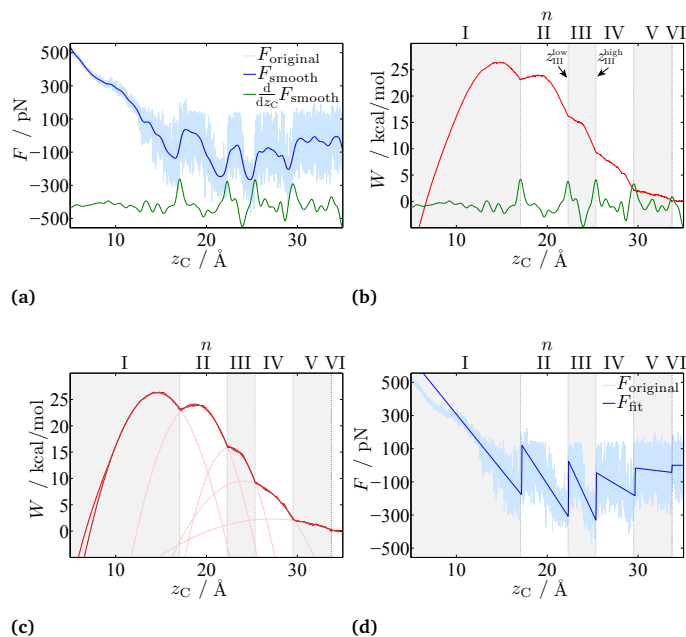


**Fig. 6** Steps of the piecewise-linear fitting procedure applied to a representative SMD force-displacement curve of GCRL desorption (see text). The corresponding fitted parameters are reported in Table 2.

normal distribution of  $k_{\text{eff}}$  is expected since the effective spring constant has to follow the same distribution of the binding forces, given the external harmonic constraint moving at constant speed. In turn, adhesion forces are very often observed to follow log-normal distributions as a consequence of the Arrhenius law governing the unbinding rate (which is the basis of the Bell-Evans model). The maximum forces are plotted as a function of the effective bond loading rates  $r_{\text{eff}} = v_{\text{pull}} \cdot k_{\text{eff}}$  in Fig. 7b, and fitted separately for each  $k_c$  value with the model of Friddle *et al.*<sup>25</sup>. This model provides a functional relationship between peak force and loading rate, having as a fixed input parameter the mean effective stiffness  $\langle k_{\text{eff}} \rangle$  and as free parameters the equilibrium force  $F_{\text{eq}}$ , the transition length  $x_t$  and the unbinding constant  $k_u^0$  associated with the surface-molecule bond.

The obtained parameters and confidence intervals for our three fits are summarized in Table 3.

We note that the values of  $x_t$  and  $k_u^0$  may be not physically relevant in this case because of the very high loading rates in the SMD simulations. In fact, the very low value of  $k_u^0$  indicates that re-binding cannot take place, as it should be for a quasi-equilibrium process and assumed in the model of Friddle *et al.*<sup>25</sup>. Nevertheless,  $x_t$  is of the typical order of magnitude of values obtained in experimental studies of biomolecular adsorption (see Tables 1 and S1 in ref. 25).

The most important parameter for our purposes is the limit of the peak forces at zero loading rate,  $F_{\text{eq}}$ , from which the adsorption free energy  $\Delta G_{\text{ads}}$  can be calculated according to Eq. 6 (see Table 3). While the adsorption free energy should be independent of the individual cantilever (or effective) spring constant, this is not fully true for the case here. This can be attributed either to the broad scattering of data points in Figure 7b or the exceed-

**Table 3** Parameters and asymptotic standard parameter errors for the model proposed by Friddle *et al.*<sup>25</sup> fitted to the data in Figure 7b, along with the corresponding values of  $\Delta G_{\text{ads}}$  obtained via Eq. 6.

$k_c / \frac{\text{pN}}{\text{\AA}}$	$\langle k_{\text{eff}} \rangle / \frac{\text{pN}}{\text{\AA}}$	$F_{\text{eq}} / \text{pN}$	$x_r / \text{\AA}$	$k_u^0 / \text{ps}^{-1}$	$\Delta G_{\text{ads}} / \frac{\text{kcal}}{\text{mol}}$
69.5	$46.5 \pm 32.1$	$230 \pm 14$	$0.28 \pm 0.03$	$0.0009 \pm 0.0004$	$-8.2 \pm 5.7$
139.0	$72.1 \pm 36.2$	$271 \pm 16$	$0.23 \pm 0.03$	$0.0015 \pm 0.0006$	$-7.3 \pm 3.7$
694.8	$122.3 \pm 47.2$	$288 \pm 15$	$0.19 \pm 0.02$	$0.0029 \pm 0.0009$	$-4.9 \pm 2.0$

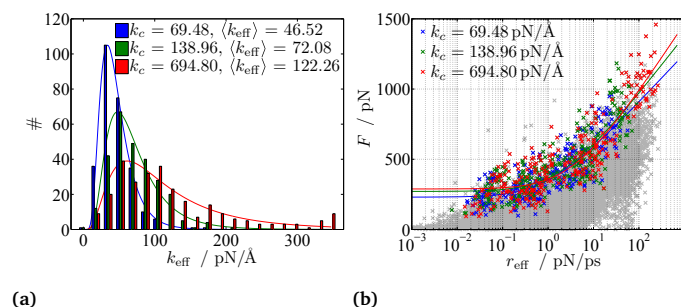


**Fig. 7** (a) Distributions of effective bond spring constants  $k_{\text{eff}}$  obtained with three different harmonic constraint stiffnesses  $k_c$  (colored bars) and their respective mean values obtained from log-normal fits (straight lines). (b) Peak forces from all performed SMD simulations as a function of the corresponding  $k_{\text{eff}}$  values. The maximum peak forces of each trajectory are indicated in colors, whereas all other identified peaks are indicated with gray crosses. The colored lines represent fits of the maximum forces with the model of Friddle *et al.*<sup>25</sup>. The obtained fitting parameters can be found in Table 3.

ingly high loading rates, which are not anymore representative of a quasi-equilibrium situation, as noted above. This would also be consistent with the shift of  $x_r$  to lower values with increasing cantilever stiffness. Moreover, a further source of uncertainty is the choice of the mean of the  $k_{\text{eff}}$  distribution, rather than for instance the median or the mode, as the representative value for  $\langle k_{\text{eff}} \rangle$ . Despite of these facts, the calculated  $\Delta G_{\text{ads}}$  are not too dissimilar to the values of -7.3 and -8.0 kcal/mol obtained with the RESTmetaD method and from the Jarzynski's Equality.

### 3.2.3 Origin of Peak Forces in the SMD Simulations

As a direct outcome of the many SMD simulation trajectories, we obtain a clear picture of which surface-molecule interactions contribute to the adsorption and are mainly responsible for the adsorption peak forces. Exemplary SMD force-retraction curves are shown in Figure 8 for different  $k_c$  and  $v_{\text{pull}}$  values together with the water density profile near the  $\text{SiO}_2$  surface and the evolution of the center of mass positions of single amino acids. Visible is a clear correlation between each peak position and the corresponding detachment of the amino acids from the surface hydration layers. The highest peak forces are mostly observed when the arginine group is released from the first hydration layer close to the surface. However, not only the breakup of the long-range electrostatic interaction between the charged arginine group and deprotonated silanol groups on the surface contribute to adhesion forces. For instance, also the trapping of non-polar residues (here, leucine) in the first water density minimum is an important contribution to the adsorption driving force, as observed in several previous works<sup>35,36,49,61</sup>. Also to be noted is that not all small

peaks resulting from the piecewise linear fitting are attributable to the breaking of surface-molecule interactions, but also to intramolecular rearrangements within the polypeptide during the pulling.

### 3.3 AFM force spectroscopy experiments

In this section we perform AFM force spectroscopy experiments to measure the desorption force of the GCRL peptide from amorphous silica in bulk liquid water. To this aim, silicon nitride AFM tips are first covalently functionalized with PEG linker molecules, to which (GCRL)<sub>15</sub> polypeptides are attached via standard condensation reactions (see Methods and Fig. 9a). The functionalized cantilevers are then approached to a fused quartz surface until surface contact is established, and are then retracted with constant velocity, leading to force-distance curves which are exemplarily shown in Fig. 9b. After an initial non-specific desorption peak arising from the detachment of the PEG-functionalized tip from the surface, a constant force plateau is observed in the majority of the measured curves. This force plateau corresponds to the progressive detachment of individual GCRL units from the surface,<sup>31,68</sup> and its height is equal to the work of adhesion per unit of length of desorbing polypeptide,<sup>33</sup> under the action of the flexible cantilever (with stiffness  $k_c$ ) and the elastic PEG linker (with stiffness  $k_{\text{PEG}}$ ).<sup>69–71</sup> In a few cases, plateaus that are much longer than the expected contour length of the combined PEG-(GCRL)<sub>15</sub> system are obtained, probably as a result of spurious agglomeration or polycondensation of more than one (GCRL)<sub>15</sub> molecule (see Fig. 9b, bottommost panel). These cases are discarded from the further analysis.

Our goal now is to extract information about the adsorption free energy from the AFM force spectroscopy experiments and, in doing so, to strive a comparison with the simulation results presented in the previous chapter. Estimates of the adsorption free energy will be obtained in two ways. First, from the model of Friddle applied to the measured adhesion forces at variable loading rates<sup>25</sup>, similarly as done with the SMD simulation results. Second, from the elastic energy contributions stored in the functionalized cantilever, the stretched PEG linker and the desorbed portion of the (GCRL)<sub>15</sub> molecule at the point of final detachment of the rest of the adsorbed (GCRL)<sub>15</sub> molecule from the surface, according to Krysiak *et al.*<sup>29</sup>. In both cases, we require details of the elasticity of the PEG linker and the (GCRL)<sub>15</sub> peptide, as presented in the next sections.

#### 3.3.1 PEG Linker Elasticity

The stretching stiffness of single PEG molecules is highly non-linear and varies with the externally applied force. The variation of the end-to-end distance  $L_{\text{ce}}^{\text{PEG}}$  of a

$$L_{\text{ee}}^{\text{PEG}}(F) = N_s \cdot \left( \frac{L_{\text{planar}}}{e^{\frac{\Delta G(F)}{k_B T}} + 1} + \frac{L_{\text{helical}}}{e^{-\frac{\Delta G(F)}{k_B T}} + 1} \right) \cdot \left( \coth \left( \frac{F \cdot L_K}{k_B T} \right) - \frac{k_B T}{F \cdot L_K} \right) + N_s \frac{F}{K_s} \quad (9)$$

$$\text{with } \Delta G(F) = (G_{\text{planar}} - G_{\text{helical}}) - F \cdot (L_{\text{planar}} - L_{\text{helical}}).$$

This model takes into account the trans-gauche transitions of the PEG backbone through (i) the lengths of the individual trans-trans-gauche and all-trans monomer conformations,  $L_{\text{helical}}$  and  $L_{\text{planar}}$ , respectively, and (ii) their associated free energies,  $G_{\text{helical}}$  and  $G_{\text{planar}}$ . Further parameters in this model are the Kuhn length of the polymer  $L_K$  and the monomer elasticity  $K_s$ , whose values have been experimentally determined<sup>69</sup> and are reported in the caption of Fig. 10.

We apply here this model to a PEG molecule consisting of 18 monomers, which roughly correspond to the length of our linker (Fig. 10). As a result, we can estimate the spring constant of the PEG linker at the typical force value of the desorption plateau observed in the force-spectroscopy experiments,  $k_{\text{PEG}} = 12.8 \text{ pN}/\text{\AA}$ . This lies within the linear force-elongation regime arising from helical unfolding of the molecule<sup>69</sup>, where the C-C bonds retain a gauche state typical for PEG dissolved in water<sup>72</sup>. It can thus be safely assumed that in this regime (between 70 and 250 pN) the PEG linker behaves like a harmonic spring.

### 3.3.2 (GCRL)<sub>15</sub> Elasticity

The elasticity of the (GCRL)<sub>15</sub> polypeptide is determined by means of the WLC model of Bouchiat *et al.*<sup>73</sup> fitted on force-elongation data obtained in a near-equilibrium SMD simulation of a shorter (GCRL)<sub>5</sub> polypeptide solvated in TIP3P water. Namely, the N-terminus and C-terminus are slowly pulled apart at a speed of  $0.1 \cdot 10^{-3} \text{ \AA}/\text{ps}$  using a harmonic constraint with a spring constant of  $20.8 \text{ pN}/\text{\AA}$ , resulting in an overall simulation time of  $2 \mu\text{s}$ . The result of this simulation is shown in Figure 11 along with the result of the WLC fitting. We note that within the applied WLC model the stretching stiffness of a (GCRL)<sub>N</sub> polymer is related to the stiffness of each individual monomer as in a series of Hookean springs:  $k_{(\text{GCRL})_N} = k_{\text{GCRL}}/N$ . Therefore, from the derivative of the force curve with respect to the end-to-end distance of (GCRL)<sub>5</sub> we can obtain both the stretching stiffness of one (GCRL) monomer,  $k_{\text{GCRL}}(F)$ , or of (GCRL)<sub>N</sub> polymers of arbitrary length, at any given force or extension value. Moreover, we can extract the end-to-end distance of a monomer at a given force value,  $L_{\text{ee}}^{\text{GCRL}}(F) = L_{\text{ee}}^{(\text{GCRL})_5}(F)/5$ .

### 3.3.3 Free Energy Estimates from Single Molecule Force Spectroscopy Measurements

The average adsorption forces obtained at variable loading rates with the PEG/(GCRL)<sub>15</sub> functionalized cantilevers are displayed in Fig. 12. Here, the loading rate is computed as the product of the cantilever pulling speed by the effective stretching stiffness of the linker system,  $r_{\text{eff}} = v_{\text{pull}} \cdot k_{\text{eff}}$ . Since the desorbing force plateau is constant during polypeptide desorption, and the

interaction between the PEG molecule and the surface is negligible, the force plateau equals the force required to detach the first GCRL monomer from the surface. For this first detaching event,  $k_{\text{eff}}$  is determined by the bending stiffness of the cantilever,  $k_c$ , the stretching stiffness of the PEG linker,  $k_{\text{PEG}}$ , and the stiffness of a GCRL monomer,  $k_{\text{GCRL}}$ :

$$\frac{1}{k_{\text{eff}}} = \frac{1}{k_c} + \frac{1}{k_{\text{PEG}}} + \frac{1}{k_{\text{GCRL}}(F)}. \quad (10)$$

In this way, the desorption of the first monomer can be interpreted as a two-state process, for which the model of Friddle can be applied<sup>30,32</sup>. Indeed, the force spectroscopy data can be well fitted with the Friddle model, using a robust Levenberg-Marquardt algorithm. The extracted parameters are  $F_{\text{eq}} = 77.5 \pm 3.0 \text{ pN}$ ,  $x_f = 0.22 \pm 0.40 \text{ \AA}$ , and  $k_u^0 = 2589 \pm 3160 \text{ s}^{-1}$  (Fig. 12). Since  $k_u^0$  is the unbinding rate at zero loading rate we consequently use  $k_{\text{eff}}(F)|_{F_{\text{eq}}}$  in our calculations. At this point, from Eq. 6 we are able to estimate an adsorption free energy for GCRL which lies between  $\Delta G_{\text{ads}} = -8.8 \pm 2.3$  and  $-7.4 \pm 2.0 \text{ kcal/mol}$ , depending on whether the GCRL stiffness is considered or not, respectively. Despite the rough approximation inherent in the application of the Friddle model to our system and in the estimation of the effective linker stiffness, this result is in reasonable agreement with our simulation estimates.

Alternatively, following the considerations of Krysiak *et al.*<sup>29</sup>, we can estimate the adsorption free energy from a balance of the elastic energy stored in the linker/cantilever system and the adsorption energy of the adsorbed portion of the peptides at the moment of the final detachment. This corresponds to the end of the plateau region in the AFM force-displacement curves (see Fig. 9). If  $N_{\text{ads}}$  and  $N_{\text{des}}$  are the number of adsorbed and desorbed GCRL monomers at the moment of detachment (with  $N_{\text{ads}} + N_{\text{des}} = 15$ ), we can write:

$$-\Delta G_{\text{ads}}^{\text{GCRL}} \cdot N_{\text{ads}} = E_c(F_{\text{eq}}) + E_{\text{PEG}}(F_{\text{eq}}) + E_{(\text{GCRL})_{N_{\text{des}}}}(F_{\text{eq}}). \quad (11)$$

Here,  $E_c(F_{\text{eq}})$  is the elastic energy stored in the bent cantilever,  $E_c(F_{\text{eq}}) = F_{\text{eq}}^2/(2 \cdot k_c) = 1.0 \text{ kcal/mol}$ . The energy stored in the stretched PEG linker is obtained by numerical integration of the inverse function given in Eq. (9) up to  $L_{\text{ee}}^{\text{PEG}}(F_{\text{eq}})$ , yielding  $E_{\text{PEG}}(F_{\text{eq}}) = 11.0 \text{ kcal/mol}$ . To calculate the energy stored in the desorbed part of the (GCRL)<sub>15</sub> polypeptide, first the amount of desorbed GCRL monomers  $N_{\text{des}}$  has to be estimated. This is done by subtracting the end-to-end length of the PEG linker at  $F_{\text{eq}}$  from the average equilibrium plateau length  $H_{\text{eq}} = 158 \pm 57 \text{ \AA}$  (Fig. 13), and dividing the result by the end-to-end length of a GCRL

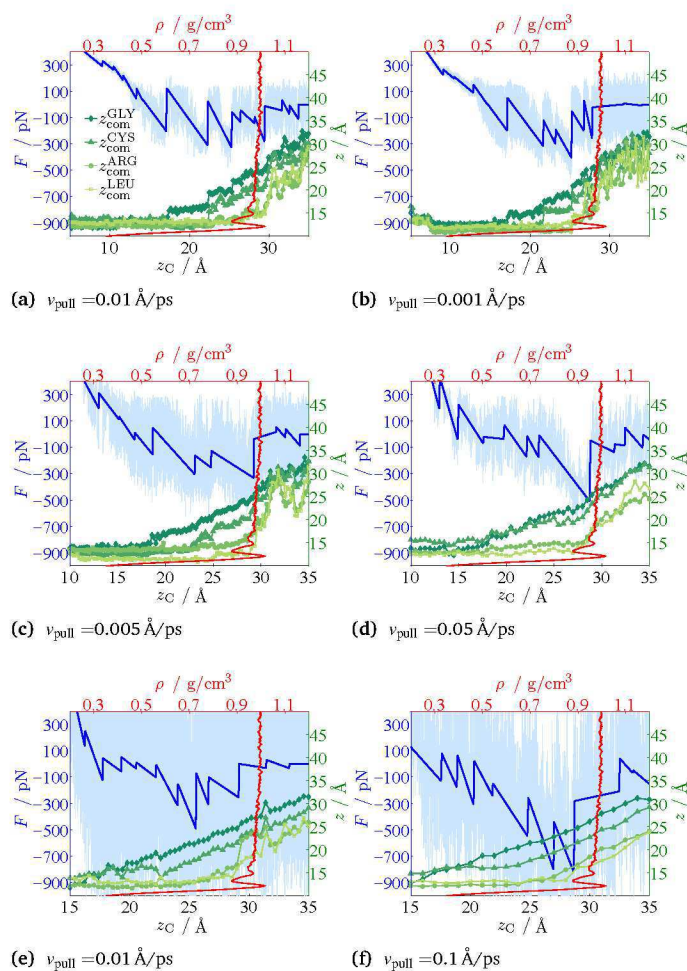


**Fig. 8** Representative SMD force-displacement curves of GCRL desorption (light blue) along with their piecewise-linear fits (blue), superimposed to the evolutions of the center-of-mass positions of selected residues (green) and the water density profile at the anionic silica surface (red). The curves are obtained for  $k_c = 694.8$  pN/Å and different pulling speeds, as indicated.

monomer,  $L_{ee}^{GCRL} = 13.4$  Å, which leads to  $N_{des}(F_{eq}) = 8.1 \pm 2.9$ . Numerical integration of the WLC model applied to a  $(GCRL)_{N_{des}}$  polymer gives  $E_{(GCRL)_{N_{des}}}(F_{eq}) = 21.7 \pm 10.2$  kcal/mol. Insertion of these quantities in Eq. 11 with  $N_{des} = 8$  and  $N_{ads} = 7$  finally leads to  $\Delta G_{ads} = -5.1 \pm 4.7$  kcal/mol.

We note here that the latter estimation of  $\Delta G_{ads}$  is strongly affected by the broad distribution of plateau end distances (Fig. 13), giving an error on the estimation of  $H_{eq}$  of the order of a few nm. Moreover, the uncertainty about the precise binding point of the PEG linker to the cantilever tip (which could be higher than the tip position) should also be considered, so that our estimate of  $H_{eq}$  is actually a lower limit for the real value. This means that so-determined absolute value of  $\Delta G_{ads}$  is also a lower limit for the true adsorption free energy. Despite of these large uncertainties and rough approximations, however, also in this case the  $\Delta G_{ads}$  agrees well with the previous estimates of this study, as summarized in Table 4.

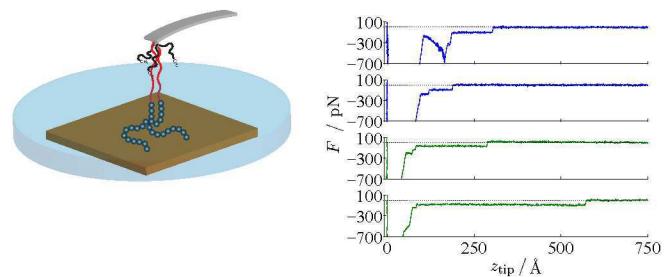


**Fig. 9** (a) Sketch of the AFM experimental setup. Black lines represent the PEG linkers capped by a methanol group and red lines the linkers bound to  $(GCRL)_{15}$  polypeptides, shown as blue-grey beads. The brown surface depicts the flat fused silica surface. (b) Typical force-displacement curves collected at different retraction speeds (green and blue for 0.1 and 0.2  $\mu\text{m/s}$ , respectively).  $z_{tip}$  is the tip-sample separation.

## 4 Discussion and Conclusions

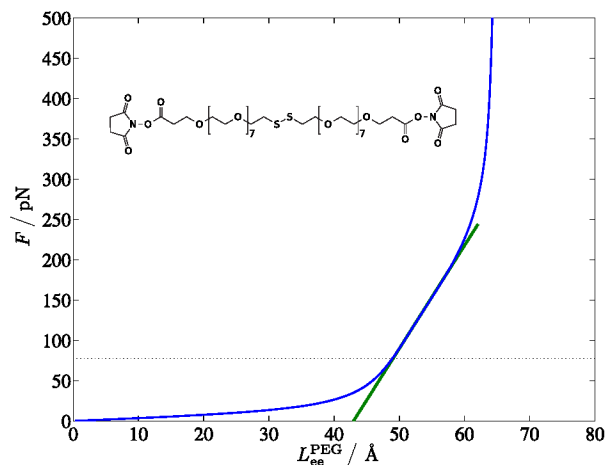
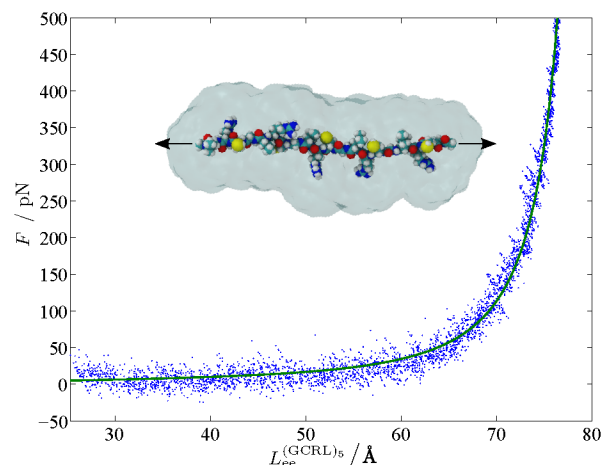
In this work we have attempted a comparison between different methods for the estimation of the adsorption free energy of short polypeptides at solid/liquid interfaces by means of both Molecular Dynamics (MD) simulations and AFM force spectroscopy experiments. As a model system, the adsorption of the (GCRL) peptide sequence on amorphous silica in contact with water at pH 7 has been considered. This sequence had been identified in a previous experimental work<sup>9</sup> as a possible (weak) binder for silica, but its surface binding affinity remained uncertain. Indeed, the results of the present investigation suggest a relatively low free energy of adsorption  $\Delta G_{ads}$  between -5 and -9 kcal/mol, depending on the method used.

Among the simulation methods employed, we believe the RESTmetaD approach<sup>35,36,44,75</sup> to be the most suitable for an accurate estimation of  $\Delta G_{ads}$ , since it is limited only by the availability of computational resources to perform simulations which are long enough to reach adequate convergence. Obviously, whether the achieved result can be trusted or not is strictly dependent on the accuracy of the employed force field, and this is an issue that will still require further comparative studies with adequately performed experiments. However, extracting accurate adsorption energy values from experimental studies of peptide adsorption is far from trivial, as it relies on the interpretation of rough data through models which may introduce large errors and uncertainties.

Dynamical force spectroscopy experiments have been widely used in the past for the investigation of surface-molecule adhesion forces, and several competing models have been developed to extract estimates of the binding free energy from measurements of adhesion forces. A particularly suitable model is the one of Friddle and De Yoreo<sup>25</sup>, in which the analytic expression linking the loading rate on the bond with the force required to break it can be readily fitted to many different non-covalently bonded systems. In order to apply the Friddle model to our case, we have consid-

**Table 4** Summarized results of the adsorption free energy obtained with various methods from simulations and experiments.

	RESTmetaD	SMD $k_c / \frac{\text{pN}}{\text{\AA}}$	JE <sup>63</sup>	Friddle <sup>25</sup>	AFM Krysiak <sup>29</sup>	Friddle <sup>25</sup>
$\Delta G_{\text{ads}} / \frac{\text{kcal}}{\text{mol}}$	$-7.3 \pm 1.8$	69.48 138.86 694.80	$-17.7 \pm 6.1$ $-16.1 \pm 5.8$ $-8.0 \pm 4.9$	$-8.2 \pm 7.2$ $-7.3 \pm 6.0$ $-4.9 \pm 3.6$	$-5.1 \pm 4.7$	$-7.4 \pm 2.0$ $-8.8 \pm 2.3$

**Fig. 10** Force-extension curve for our PEG linker molecule (inset) calculated with the model of Oesterhelt *et al.*<sup>69</sup> (blue) (Eq. (9)). Model parameters are as follows:  $N_s = 18$ ,  $K_s = 150 \text{ N/m}$ ,  $G_{\text{planar}} - G_{\text{helical}} = 3 k_B T$ ,  $L_{\text{planar}} = 3.6 \text{ \AA}$ ,  $L_{\text{helical}} = 2.8 \text{ \AA}$ ,  $L_K = 7 \text{ \AA}$ . A linear segment (green) is fitted to the supramolecular recognition force regime region to estimate the elasticity of the linker at typical measured desorption forces (dotted line).**Fig. 11** WLC model of Marko and Siggia<sup>74</sup> (green curve) fitted to SMD data (blue dots) of a (GCRL)<sub>5</sub> polypeptide extended in TIP3P water (inset). The persistence length and contour length are estimated to 4.15 Å and 82.14 Å, respectively.

ered the elasticity of the PEG linker molecule and of the GCRL polypeptide itself, and obtained a rough estimate of the free energy of binding that is in reasonable agreement with the RESTmetaD reference (Table 4). We have also applied the same model to three sets of simulation data obtained via Steered MD. This has required the development of a procedure to reliably extract force peaks from noisy force-distance curves obtained in a large number of MD trajectories, after subtraction of the friction work arising from pulling the peptide through water at very high speed (see Fig. 6). Our newly developed procedure gives both information on the peak forces and on the effective spring constant acting on each surface molecule bond, and thus on the effective bond loading rates. Especially applying intermediate harmonic springs to pull the molecule off the surface results in estimates of both the adsorption free energy and of the bond breaking transition length in very good agreement with the corresponding experimental estimates ( $-7.3$  vs  $-7.4$  eV -and  $0.23$  vs  $0.22$  Å, respectively). The agreement is impressive given the several orders of magnitude difference in the typical loading rates of the experiments ( $10^3$  to  $10^6$  pN/s) and simulations ( $10^{10}$  to  $10^{14}$  pN/s). However, this is well reflected in the fitted value of the unbinding constant  $k_u^0$  ( $2.6 \text{ ms}^{-1}$  in the experiments,  $1.5 \text{ ns}^{-1}$  in the simulations), which is dictated by the pulling speed in the latter case. This means that in the simulations we are actually out of equilibrium, so that the application of the Friddle model shall be performed with care and without giving a strong physical meaning to the fitted kinetic

constant values<sup>34</sup>.

More appropriate in this case is the direct use of the Jarzynski's Equality<sup>63</sup> to extract the free energy of adsorption from SMD simulations. This method relies on the stochastic presence of small work values to detach the molecule from the surface, which are essential for a robust free energy estimate. Therefore, it is not sufficient to use starting adsorption configurations where the peptide is in a few deep local minima, but to use a large number of independent (although realistic) configurations. We have achieved this in an ideal way by repeatedly pushing and pulling the probe molecule towards and off the surface with the help of appropriate harmonic constraints, which effectively mimics AFM force-spectroscopy experiments. However, as expected, the convergence of the free energy values with the pulling speed is only very rough (see Fig. 5), and a  $\Delta G_{\text{ads}}$  value in reasonable agreement with the RESTmetaD reference is only obtained for the stiffest spring and the lowest pulling speed employed.

Finally, the force-spectroscopy experiments have been also interpreted in terms of an energy balance between the adsorption free energy of the biomolecule and the elastic energy stored in the cantilever system. In this case, the main limitation of the method is the uncertainty about the precise contour length of the PEG linker due to the random attachment position to the AFM cantilever on the one side and the extremely wide distribution of measured detaching lengths on the other side. While an accurate model has been developed to deal with this situation for the case of negligible surface-molecule friction<sup>29</sup>, the model is not directly applicable to our case of a polypeptide in contact with an oxide

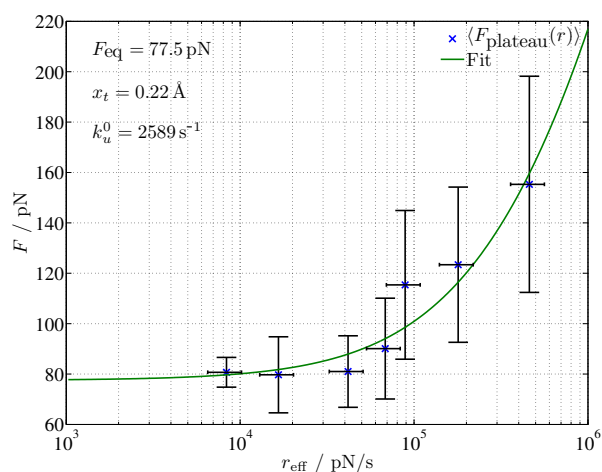


**Fig. 12** Average plateau forces of the (GCRL)<sub>15</sub> polypeptide on silica measured by AFM force spectroscopy at several loading rates. The fit with the model of Friddle *et al.*<sup>25</sup> is shown as a straight line, and the fitting parameters are reported in the inset.

surface. The fact that we obtain a very reasonable estimate of the free energy also in this case should be considered as almost fortuitous, as indicated by the very large error bar associated with it.

In conclusion, while advanced molecular dynamics simulations can be used to achieve very precise estimates of the surface-molecule adsorption free energy within a given force field, experimental determination of the same quantity by means of dynamic force spectroscopy is still associated with large uncertainties. The available models shall be extended both to take into account strong surface-molecule friction and to remove the explicit dependence of quantities that are not readily experimentally accessible, such as the contour length of the linker. In further works comparisons to other experimental approaches, such as quartz crystal microbalance or isothermal titration calorimetry, which can be performed with short peptide sequences, should also be attempted.

## Acknowledgements

The authors are grateful to Tiffany Walsh (Deakin University, Australia), Robert Latour (Clemson University, USA) and Stefano Corni (University of Modena, Italy) for stimulating discussions. We also acknowledge fruitful suggestions by Jakob Tómas Bullerjahn (University of Leipzig, Germany) and Raymond W. Friddle (Sandia National Laboratories, USA). This work has been funded by the DFG under Grant CI/144-2 (Emmy Noether Programme) and the European Commission via the FP7-NMP Grant 229205 “ADGLASS”. Computational Resources have been provided by the Fraunhofer Gesellschaft and the North-German Supercomputing Alliance system (HLRN).

## References

- 1 S. R. Couto and J. L. T. Herrera, *Biotechnol. Adv.*, 2006, **24**, 500–513.
- 2 J. E. Moses and A. D. Moorhouse, *Chem. Soc. Rev.*, 2007, **36**,

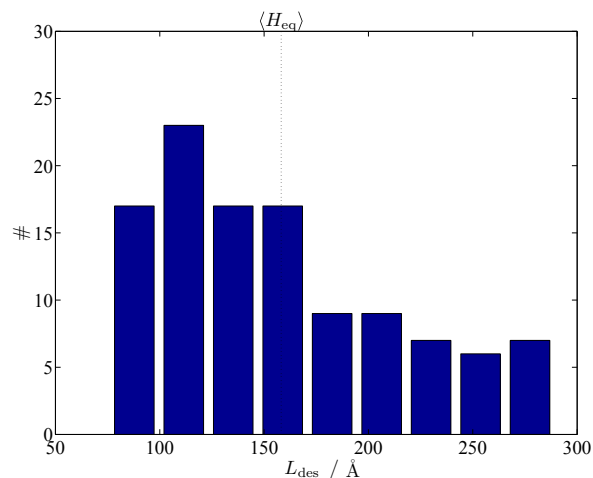


**Fig. 13** Distribution of the plateau lengths for (GCRL)<sub>15</sub> desorption from silica, as measured with AFM force spectroscopy at the three smallest loading rate values in Fig. 12. The mean plateau length is estimated to  $H_{eq} = 158\text{Å}$ .

1249–1262.

- 3 J. Lv, Y. Song, L. Jiang and J. Wang, *ACS Nano*, 2014, **8**, 3152–3169.
- 4 E. Müller, Werner, X. Wang, P. Proksch, C. Perry, Carole, R. Osinga, J. Gardères and C. Schröder, Heinz, *Mar. Biotechnol.*, 2013, **15**, 375–398.
- 5 I. Banerjee, R. C. Pangule and R. S. Kane, *Adv. Mater. (Weinheim, Ger.)*, 2011, **23**, 690–718.
- 6 C. Tamerler and M. Sarikaya, *ACS Nano*, 2009, **3**, 1606–1615.
- 7 Z. Tang, J. P. Palafox-Hernandez, W.-C. Law, Z. E. Hughes, M. T. Swihart, P. N. Prasad, M. R. Knecht and T. R. Walsh, *ACS Nano*, 2013, **7**, 9632–9646.
- 8 S. Corni, M. Hnilova, C. Tamerler and M. Sarikaya, *J. Phys. Chem. C*, 2013, **117**, 16990–17003.
- 9 S. Steckbeck, J. Schneider, L. Wittig, K. Rischka, I. Grunwald and L. C. Ciacchi, *Anal. Methods*, 2014, **6**, 1501.
- 10 M. Rabe, D. Verdes and S. Seeger, *Adv. Colloid Interface Sci.*, 2011, **162**, 87–106.
- 11 V. P. Raut, M. A. Agashe, S. J. Stuart and R. A. Latour, *Langmuir*, 2005, **21**, 1629–1639.
- 12 E. E. Oren, R. Notman, I. W. Kim, J. S. Evans, T. R. Walsh, R. Samudrala, C. Tamerler and M. Sarikaya, *Langmuir*, 2010, **26**, 11003–11009.
- 13 D. Horinek, A. Serr, M. Geisler, T. Pirzer, U. Slotta, S. Q. Lud, J. A. Garrido, T. Scheibel, T. Hugel and R. R. Netz, *Proc. Natl. Acad. Sci. U. S. A.*, 2008, **105**, 2842–2847.
- 14 O. Cohavi, S. Corni, F. De Rienzo, R. Di Felice, K. E. Gottschalk, M. Hoefling, D. Kokh, E. Molinari, G. Schreiber, A. Vaskevich and R. C. Wade, *J. Mol. Recognit.*, 2010, **23**, 259–262.
- 15 Y. Wei and R. A. Latour, *Langmuir*, 2008, **24**, 6721–6729.
- 16 A. Serro, K. Degiampietro, R. Colaço and B. Saramago, *Colloids Surf., B*, 2010, **78**, 1–7.
- 17 C. Kößlinger, E. Uttenthaler, S. Drost, F. Aberl, H. Wolf,

- G. Brink, A. Stanglmaier and E. Sackmann, *Sens. Actuators, B*, 1995, **24**, 107–112.
- 18 J. Kim, S. Kim, T. Ohashi, H. Muramatsu, S.-M. Chang and W.-S. Kim, *Bioprocess Biosyst. Eng.*, 2010, **33**, 39–45.
- 19 P. Ansorena, A. Zuzuarregui, E. Pérez-Lorenzo, M. Mujika and S. Arana, *Sens. Actuators, B*, 2011, **155**, 667–672.
- 20 A. A. Thyparambil, Y. Wei and R. A. Latour, *Langmuir*, 2012, **28**, 5687–5694.
- 21 Y. Wei and R. A. Latour, *Langmuir*, 2010, **26**, 18852–18861.
- 22 K. C. Neuman and A. Nagy, *Nat. Methods*, 2008, **5**, 491–505.
- 23 N. Varghese, U. Mogera, A. Govindaraj, A. Das, P. K. Maiti, A. K. Sood and C. N. R. Rao, *ChemPhysChem*, 2009, **10**, 206–210.
- 24 E. Evans and K. Ritchie, *Biophys. J.*, 1997, **72**, 1541–1555.
- 25 R. W. Friddle, A. Noy and J. J. De Yoreo, *Proc. Natl. Acad. Sci. U. S. A.*, 2012, **109**, 13573–13578.
- 26 O. K. Dudko, G. Hummer and A. Szabo, *Phys. Rev. Lett.*, 2006, **96**, 108101.
- 27 O. K. Dudko, G. Hummer and A. Szabo, *Proc. Natl. Acad. Sci. U. S. A.*, 2008, **105**, 15755–15760.
- 28 F. Rico, L. Gonzalez, I. Casuso, M. Puig-Vidal and S. Scheuring, *Science*, 2013, **342**, 741–743.
- 29 S. Krysiak, S. Liese, R. R. Netz and T. Hugel, *J. Am. Chem. Soc.*, 2014, **136**, 688–697.
- 30 F. T. Hane, S. J. Attwood and Z. Leonenko, *Soft Matter*, 2014, **10**, 1924–1930.
- 31 S. Iliafar, K. Wagner, S. Manohar, A. Jagota and D. Vezenov, *J. Phys. Chem. C*, 2012, **116**, 13896–13903.
- 32 S. Iliafar, D. Vezenov and A. Jagota, *Langmuir*, 2013, **29**, 1435–1445.
- 33 J. Paturej, J. L. A. Dubbeldam, V. G. Rostiashevili, A. Milchev and T. A. Vilgis, *Soft Matter*, 2014, **10**, 2785–2799.
- 34 J. T. Bullerjahn, S. Sturm and K. Kroy, *Nat. Commun.*, 2014, **5**, 1–10.
- 35 J. Schneider and L. Colombi Ciacchi, *J. Am. Chem. Soc.*, 2012, **134**, 2407–2413.
- 36 R. H. Meißner, J. Schneider, P. Schiffels and L. Colombi Ciacchi, *Langmuir*, 2014, **30**, 3487–3494.
- 37 R. Di Felice and S. Corni, *J. Phys. Chem. Lett.*, 2011, **2**, 1510–1519.
- 38 C. P. O'Brien, S. J. Stuart, D. A. Bruce and R. A. Latour, *Langmuir*, 2008, **24**, 14115–14124.
- 39 H. Fukunishi, O. Watanabe and S. Takada, *J. Chem. Phys.*, 2002, **116**, 9058–9067.
- 40 Y. Sugita and Y. Okamoto, *Chem. Phys. Lett.*, 1999, **314**, 141–151.
- 41 P. Liu, B. Kim, R. A. Friesner and B. J. Berne, *Proc. Natl. Acad. Sci. U. S. A.*, 2005, **102**, 13749–13754.
- 42 L. Wang, R. A. Friesner and B. J. Berne, *J. Phys. Chem. B*, 2011, **115**, 9431–9438.
- 43 A. Laio and F. L. Gervasio, *Rep. Prog. Phys.*, 2008, **71**, 126601.
- 44 C. Camilloni, D. Provasi, G. Tiana and R. A. Broglia, *Proteins: Struct., Funct., Bioinf.*, 2008, **71**, 1647–1654.
- 45 D. L. Beveridge and F. M. DiCapua, *Annu. Rev. Biophys. Biophys. Chem.*, 1989, **18**, 431–492.
- 46 I. Kosztin, B. Barz and L. Janosi, *J. Chem. Phys.*, 2006, **124**, 064106.
- 47 D. J. Cole, M. C. Payne, G. Csányi, S. M. Spearing and L. Colombi Ciacchi, *J. Chem. Phys.*, 2007, **127**, 204704.
- 48 L. Colombi Ciacchi, D. J. Cole, M. C. Payne and P. Gumbsch, *J. Phys. Chem. C*, 2008, **112**, 12077–12080.
- 49 D. J. Cole, M. C. Payne and L. C. Ciacchi, *Phys. Chem. Chem. Phys.*, 2009, **11**, 11395–11399.
- 50 A. Butenuth, G. Moras, J. Schneider, M. Koleini, S. Köppen, R. Meißner, L. B. Wright, T. R. Walsh and L. C. Ciacchi, *Phys. Status Solidi B*, 2012, **249**, 292–305.
- 51 C. Jarzynski, *Phys. Rev. Lett.*, 1997, **78**, 2690–2693.
- 52 H. J. Butt and M. Jaschke, *Nanotechnology*, 1995, **6**, 1–7.
- 53 E.-L. Florin, M. Rief, H. Lehmann, M. Ludwig, C. Dornmair, V. Moy and H. Gaub, *Biosens. Bioelectron.*, 1995, **10**, 895–901.
- 54 S. Plimpton, *J. Comput. Phys.*, 1995, **117**, 1–19.
- 55 W. D. Cornell, P. Cieplak, C. I. Bayly, I. R. Gould, K. M. Merz, D. M. Ferguson, D. C. Spellmeyer, T. Fox, J. W. Caldwell and P. A. Kollman, *J. Am. Chem. Soc.*, 1995, **117**, 5179–5197.
- 56 Y. Duan, C. Wu, S. Chowdhury, M. C. Lee, G. Xiong, W. Zhang, R. Yang, P. Cieplak, R. Luo, T. Lee, J. Caldwell, J. Wang and P. Kollman, *J. Comput. Chem.*, 2003, **24**, 1999–2012.
- 57 W. L. Jorgensen, J. Chandrasekhar, J. D. Madura, R. W. Impey and M. L. Klein, *J. Chem. Phys.*, 1983, **79**, 926–935.
- 58 E. Demiralp, T. Çağın and W. A. Goddard, *Phys. Rev. Lett.*, 1999, **82**, 1708–1711.
- 59 S. H. Behrens and D. G. Grier, *J. Chem. Phys.*, 2001, **115**, 6716–6721.
- 60 M. Barisik, S. Atalay, A. Beskok and S. Qian, *J. Phys. Chem. C*, 2014, **118**, 1836–1842.
- 61 N. Hildebrand, S. Köppen, L. Derr, K. Li, M. Koleini, K. Rezwan and L. Colombi Ciacchi, *J. Phys. Chem. C*, 2015, **119**, 7295–7307.
- 62 M. Balsara, S. Stepaniants, S. Izrailev, Y. Oono and K. Schulten, *Biophys. J.*, 1997, **73**, 1281–1287.
- 63 S. Park, F. Khalili-Araghi, E. Tajkhorshid and K. Schulten, *J. Chem. Phys.*, 2003, **119**, 3559.
- 64 J. Liphardt, *Science*, 2002, **296**, 1832–1835.
- 65 G. Hummer and A. Szabo, *Proc. Natl. Acad. Sci. U. S. A.*, 2001, **98**, 3658–3661.
- 66 H. Grubmüller, B. Heymann and P. Tavan, *Science*, 1996, **271**, 997–999.
- 67 A. Maitra and G. Arya, *Phys. Rev. Lett.*, 2010, **104**, 108301.
- 68 S. Manohar, A. R. Mantz, K. E. Bancroft, C.-Y. Hui, A. Jagota and D. V. Vezenov, *Nano Lett.*, 2008, **8**, 4365–4372.
- 69 F. Oesterhelt, M. Rief and H. E. Gaub, *New J. Phys.*, 1999, **1**, 6–6.
- 70 H. Kreuzer, S. Payne and L. Livadaru, *Biophys. J.*, 2001, **80**, 2505–2514.
- 71 E. Thormann, P. L. Hansen, A. C. Simonsen and O. G. Mouritsen, *Colloids Surf., B*, 2006, **53**, 149–156.

- 72 R. Begum and H. Matsuura, *J. Chem. Soc., Faraday Trans.*, 1997, **93**, 3839–3848.
- 73 C. Bouchiat, M. Wang, J.-F. Allemand, T. Strick, S. Block and V. Croquette, *Biophys. J.*, 1999, **76**, 409–413.
- 74 J. F. Marko and E. D. Siggia, *Macromolecules*, 1995, **28**, 8759–8770.
- 75 A. Gil-Ley and G. Bussi, *J. Chem. Theory Comput.*, 2015, **11**, 1077–1085.

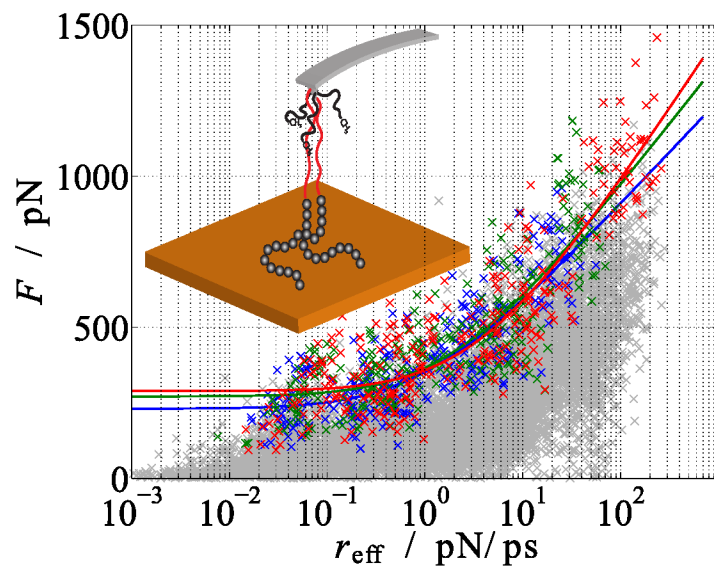


Figure 1: Combination of AFM-force spectroscopy and SMD simulations to assess the free energy of adsorption of a (poly)tetrapeptide on a silica surface.